ACSNANO
www.acsnano.org
ARTICLE

Precise Coating of a Wide Range of DNA Templates by a Protein Polymer with a DNA Binding Domain

Armando Hernandez-Garcia,[*,#,†] Nicole A. Estrich,[‡] Marc W. T. Werten,[§] Johan R. C. Van Der Maarel,[∥] Thomas H. LaBean,[‡] Frits A. de Wolf,[§] Martien A. Cohen Stuart,[†] and Renko de Vries[*,†]

[†]Physical Chemistry and Soft Matter, Wageningen University and Research, Stippeneng 4, 6708 WE Wageningen, The Netherlands
[‡]Department of Materials Science and Engineering, North Carolina State University, Raleigh, North Carolina 27695, United States
[§]Wageningen UR Food and Biobased Research, Wageningen University and Research, Bornse Weilanden 9, 6708 WG, Wageningen, The Netherlands
[∥]Department of Physics, National University of Singapore, 2 Science Drive 3, 117542 Singapore

Supporting Information

ABSTRACT: **Emerging DNA-based nanotechnologies would benefit from the ability to modulate the properties (*e.g.*, solubility, melting temperature, chemical stability) of diverse DNA templates (single molecules or origami nanostructures) through controlled, self-assembling coatings. We here introduce a DNA coating agent, called C_8–B^{Sso7d}, which binds to and coats with high specificity and affinity, individual DNA molecules as well as folded origami nanostructures. C_8–B^{Sso7d} coats and protects without condensing, collapsing or destroying the spatial structure of the underlying DNA template. C_8–B^{Sso7d} combines the specific nonelectrostatic DNA binding affinity of an archeal-derived DNA binding domain (Sso7d, 7 kDa) with a long hydrophilic random coil polypeptide (C_8, 73 kDa), which provides colloidal stability (solubility) through formation of polymer brushes around the DNA templates. C_8–B^{Sso7d} is produced recombinantly in yeast and has a precise (but engineerable) amino acid sequence of precise length. Using electrophoresis, AFM, and fluorescence microscopy we demonstrate protein coat formation with stiffening of one-dimensional templates (linear dsDNA, supercoiled dsDNA and circular ssDNA), as well as coat formation without any structural distortion or disruption of two-dimensional DNA origami template. Combining the programmability of DNA with the nonperturbing precise coating capability of the engineered protein C_8–B^{Sso7d} holds promise for future applications such as the creation of DNA–protein hybrid networks, or the efficient transfection of individual DNA nanostructures into cells.**

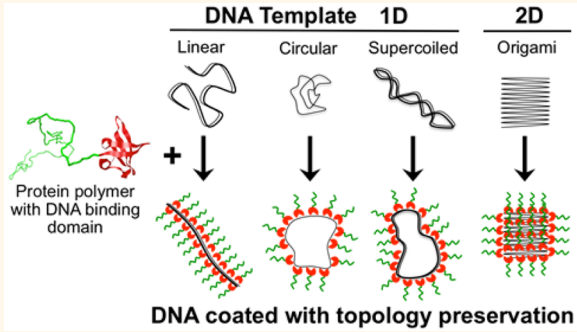

KEYWORDS: *directed self-assembly, protein engineering, DNA nanotechnology, single molecule, protein polymer, nanomaterials*

New DNA nanotechnologies such as those based on DNA origami,[1−4] single molecule DNA imaging,[5] single molecule sequencing strategies such as optical mapping,[6−9] and nanopore sequencing[10,11] increasingly rely on precise control of physical-chemical properties of individual DNA molecules: mechanical properties, interactions with nanoscale environments,[12] *etc.* While there is some opportunity to exert control *via* tuning of solution conditions, many cases exist in which incompatible solution conditions greatly hinder the ability to achieve high assembly yields for products containing diverse building materials. We expect that much higher levels of control and greater assembly yields can be obtained by developing dedicated nonelectrostatic DNA binders capable of modulating specific DNA properties. A general toolbox of DNA binders that modulate physical properties of individual DNA molecules may therefore be expected to be useful for a wide range of DNA-based technologies.

With this in mind, we have recently designed, produced and characterized a recombinant, protein-based polymer that coats individual double-stranded DNA (dsDNA) molecules and significantly increases its persistence length.[13] The polymer coating protects against enzymatic degradation without making the DNA completely inaccessible to strong (sequence specific) binders. It is composed of two polypeptide domains and its

Received: September 2, 2016
Accepted: December 1, 2016
Published: December 1, 2016

DOI: 10.1021/acsnano.6b05938
ACS Nano 2017, 11, 144−152

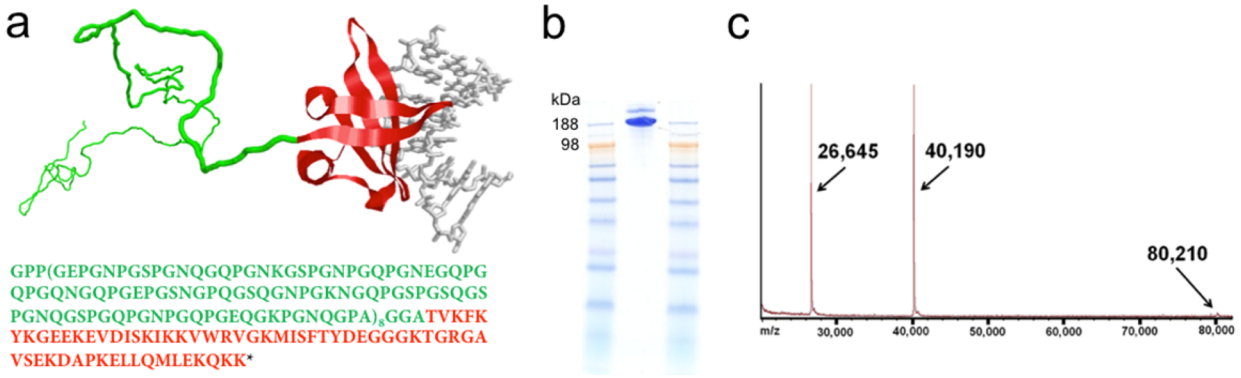

Figure 1. Protein design for DNA coating with topology preservation. (a) Schematic representation of the structure of the protein-based polymer C_8–B^{Sso7d} bound to double stranded DNA (dsDNA). In green: the hydrophilic unstructured C_8 polypeptide, in red: the B^{Sso7d} DNA-binding domain, in gray: dsDNA. The structure of B^{Sso7d} bound to dsDNA is taken from the X-ray crystallographic structure of Sso7d (pdb: 1BNZ).[17] The bottom panel gives the amino acid sequence of the C_8–B^{Sso7d} protein polymer. In green: the hydrophilic unstructured C_8 polypeptide, in red: the B^{Sso7d} DNA-binding domain. Molecular characterization of purified C_8–B^{Sso7d} by (b) SDS-PAGE. The left and right lanes are molecular weight markers, the middle lane is C_8–B^{Sso7d} after a single ammonium sulfate bulk purification step. The mobility of the main C_8–B^{Sso7d} band corresponds to a molecular weight of around 190 kDa as compared to the markers. The deviation from the real molecular weight of around 80 kDa is due to the low SDS binding of the large C_8 domain. (c) MALDI-TOF shows three peaks corresponding to the expected molecular weight for C_8–B^{Sso7d}: M^+ (80 210 Da), M^{2+} (40 190 Da) and M^{3+} (26 645 Da).

sequence is abbreviated as C_4–B^{K12}. The C_4 domain is a tetramer of a previously published collagen-inspired sequence C, a 99 amino acid polypeptide that is highly hydrophilic and forms soluble random coils over a wide range of solution conditions.[14] As a DNA binding domain, a simple stretch of 12 lysines was used (K12). The enhanced DNA stiffness provided by the C_4–B^{K12} polymer coating has already been shown to be useful for nanochannel-based optical mapping of DNA, where it allows for full stretching of DNA in rather wide nanochannels (250 × 250 nm).[8] While highly effective in coating linear dsDNA, we show here that the C_4–B^{K12} polymer causes undesirable distortion of DNA origami structures.

As a DNA binding domain, the K_{12} oligolysine domain is nonspecific. Virtually all anticipated applications of DNA binders that modulate specific DNA properties involve complicated background solutions composed of biopolymers other than DNA, and the oligolysine domain may also bind to those molecules. The same of course holds for most synthetic polycationic blocks currently used for nonviral gene transfer such as Poly-Lys, PEI or PDMAEMA. A logical next step is therefore to replace nonspecific polycationic binding blocks with nucleic acid-specific binding domains. Here we choose the 7 kDa DNA-binding protein Sso7d of the hyperthermophilic archaeabacterium *Sulfolobus solfataricus* as a nonsequence-specific nucleic acid binding domain. The binding characteristics of Sso7d to both dsDNA and ssDNA have been well characterized.[15−20] It is a highly stable protein and has been extensively used in protein engineering both in fusion constructs, and as a scaffold structure. For example, non-sequence-specific DNA binding by Sso7d has been used to improve processivity of DNA polymerases[21] and as a structural scaffold to generate highly stable binding proteins[22,23]

We here produce and study the properties of a fusion of Sso7d with a very long shielding and solubilization domain: an octamer of the 99 amino acid C-domain mentioned above. The C_8–B^{Sso7d} protein-based polymer is produced in high yield by secreted expression in the yeast *Pichia pastoris*. We study DNA stiffening and protection by coating with C_8–B^{Sso7d}, for dsDNA, ssDNA, DNA origami. Our study highlights how engineered protein-based polymers can be used in fusions with folded biological domains to construct protein-based polymers with new abilities to modulate the physical properties of DNA for a variety of applications of DNA-based technology.

RESULTS AND DISCUSSION

Protein Design and Production. The amino acid sequence of the C_8–B^{Sso7d} protein-based polymer and a cartoon of it bound to dsDNA is shown in Figure 1a, where we have used the published X-ray crystallographic structure of Sso7d bound to a short DNA double helix.[17] Note the large asymmetry of the polymer in terms of the domain lengths (63 amino acids for the B^{Sso7d} binding domain and 797 amino acids for the hydrophilic C_8 domain). The addition of a larger C-block to Sso7d than K12 aims to increase the solubility and rigidity of resultant protein−DNA complexes without affecting the nature of the interaction between protein and DNA, which is driven solely by the binding block. The C_8–B^{Sso7d} protein-based polymer, with a predicted molar mass of 80 372 Da, was successfully produced by *Pichia pastoris* as a secreted protein at an approximate yield (purified protein to volume of filtered, cell-free medium) of 0.72 g/L. Secretion of the DNA binding domain linked to the unstructured polypeptide region was well tolerated by the *P. pastoris* cells suggesting that production of other large engineered protein-based polymers is also attainable. Bulk purification using ammonium sulfate precipitation was sufficient to separate the secreted protein polymers from most other proteins secreted in the extracellular medium, as shown by SDS-PAGE in Figure 1b. Multimers of the hydrophilic C-domain are known to poorly bind SDS and hence move with anomalously low speeds in SDS-PAGE.[14] Indeed, the apparent molar mass of the purified polypeptides as deduced from electrophoretic mobility would be around 190 kDa. The molar mass of the purified protein was analyzed by MALDI-TOF mass spectrometry (Figure 1c), which shows three peaks that correspond to the M^+ (80 210 Da), M^{2+} (40 190 Da) and M^{3+} (26 645 Da) ions. This agrees with the predicted molar mass of 80 372 Da within experimental accuracy. Furthermore, the existence of the protein in a monomer state in solutions of the purified biosynthesized protein was demonstrated by Dynamic Light Scattering by

DOI: 10.1021/acsnano.6b05938
ACS Nano 2017, 11, 144−152

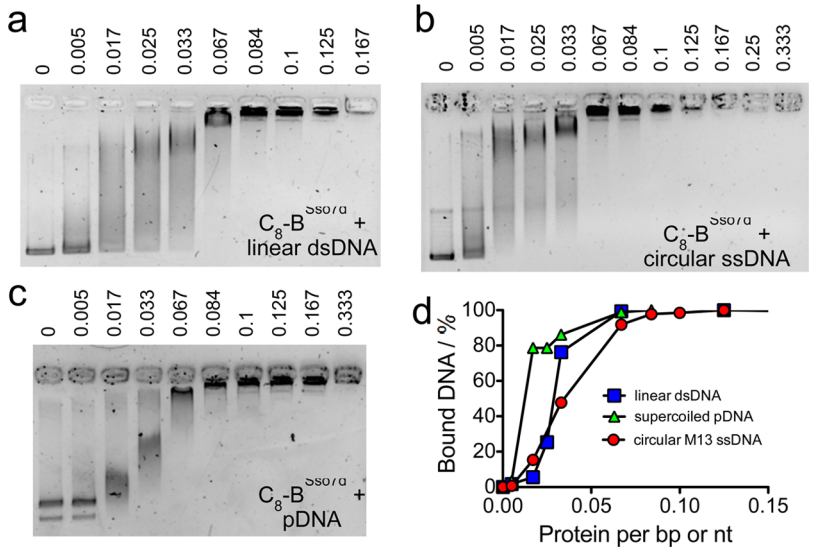

Figure 2. C_8–B^{Sso7d} binding of one-dimension DNA templates. Electrophoretic Mobility Shift Assay for (a) 2.0 kbp linear dsDNA, (b) circular M13 ssDNA and (c) 2.6 kbp pDNA complexed with C_8–B^{Sso7d}. Protein/DNA bp or nt ratio is shown at the top. (d) Plot of bound DNA as a function of protein/DNA bp ratio for dsDNA and Protein/DNA nt ratio for ssDNA.

detection of a single molecule population with a hydrodynamic radius of 7.9 nm, as expected for a hydrophilic polypeptide coil of approximately 860 amino acids.

Protein Polymer Binding Isotherms for Different Types of DNA Templates. In order to probe the DNA binding properties of C_8–B^{Sso7d} for different types of DNA templates we characterize the mobility shift with agarose gel electrophoresis (Figure 2) after the addition of C_8–B^{Sso7d} to 2.0 kbp linear DNA, 2.6 kbp supercoiled pDNA and 7249 nt circular ssDNA from M13mp18 virus (the scaffold typically used in the production of DNA origami) since Sso7d is reported to also bind to ssDNA.[24] We find that the addition of C_8–B^{Sso7d} reduces the electrophoretic mobility of all DNA templates, confirming the interaction of the protein with these DNA templates. The shift in mobility follows a similar trend for each sample. The mobility begins to decrease at a low protein/DNA ratio, 0.017 protein molecules per base pair (ptn/bp) for linear dsDNA and pDNA or per nucleotide (ptn/nt) for ssDNA. The mobility shift saturates at around 0.067 ptn/bp or ptn/nt. Higher protein concentrations do not lead to further changes in the observed mobility (see Supporting Information Figure S1) but do appear to cause a reduction in staining efficiency due to competition with the binding of the DNA stain. In contrast, using the C_4–B^{K12} protein polymer that binds to DNA purely *via* nonspecific electrostatic interactions, required the addition of a much larger excess amount of protein polymers (>0.667 ptn/bp) to achieve a complete saturation of binding as deduced from the electrophoretic mobility, as we also reported previously.[13] Structural and crystallographic studies report that B^{Sso7d} binds to dsDNA every 4 bp, equivalent to 0.25 ptn/bp.[17,25] We find that binding to dsDNA saturates at around 0.084 ptn/bp or nt, which is equivalent of one protein every 12 bp or nt. Presumably, steric interactions of the large C_8 domains prevent the coating from achieving higher densities.

Since the Sso7d domain has a tryptophan residue in the binding site, we probed the interaction between tryptophan with the dsDNA through its fluorescence quenching. In Figure 3 can be appreciated that, when excited at 285 nm, the fluorescence intensity emitted at 340 nm by tryptophan is

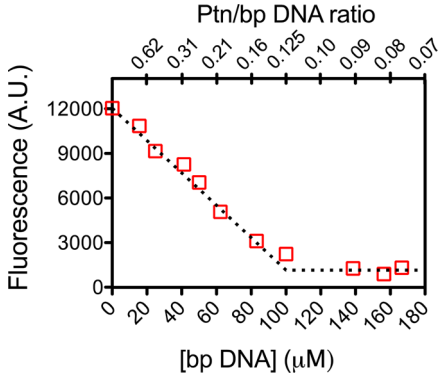

Figure 3. Fluorescence quenching of the tryptophan of the Sso7d domain by dsDNA. C_8–B^{Sso7d} concentration was 12.46 μM dissolved in 10 mM phosphate buffer pH 7.4. λ_{ex} = 285 nm and λ_{em} = 340 nm.

reduced linearly upon addition of nucleic acid. The fluorescence intensity reached a minimum at protein/DNA bp <0.09, which is in good agreement with the observed results by agarose gel electrophoresis for dsDNA (Figure 2a). This confirms the interaction between C_8–B^{Sso7d} and the DNA.

Secondary Structure of Sso7d Domain in the Context of C_8–B^{Sso7d} Protein Polymer. In order assess whether Sso7d folding is influenced by the attachment of the C_8-block, we carried out circular dichroism spectroscopy (see Supporting Information Figure S2). We use a C_4 protein polymer to obtain a reference spectrum and subtracted twice the C_4 spectrum from the spectrum of the full length C_8–B^{Sso7d} (on a molar basis), to obtain the spectrum of the Sso7d block in the context of the C_8–B^{Sso7d} protein polymer. Despite the large noise due to the large mass of the C_8-block in comparison to that of the Sso7d block, we find a difference spectrum that is very similar to those previously reported for free Sso7d.[18] Additionally, considering that the tryptophan of the binding domain Sso7d is actually interacting with those of dsDNA (Figure 3), we can conclude that the folding and interaction with DNA of the domain Sso7d is not significantly undermined by the fusion to the C_8-block.

DOI: 10.1021/acsnano.6b05938
ACS Nano 2017, 11, 144–152

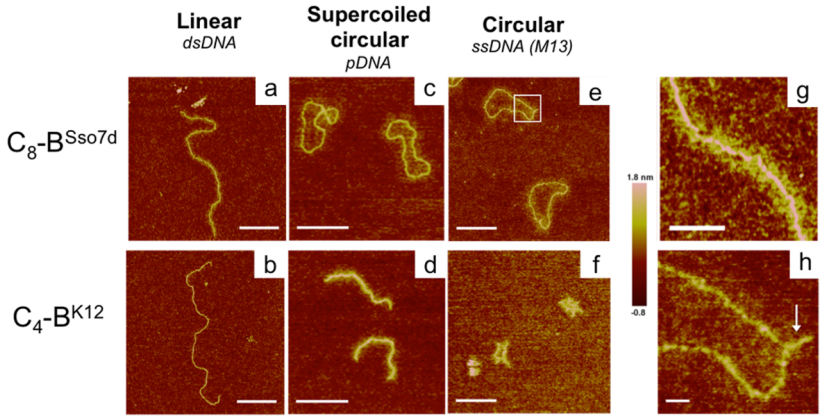

Figure 4. Comparison of structures of complexes with C_8–B^{Ssso7d} and C_4–B^{K12} protein polymers for different types of DNA templates. AFM images of dried complexes. (a,b) 8.0 kbp linear dsDNA coated with 0.125 ptn/bp of (a) C_8–B^{Sso7d} and (b) 0.125 ptn/bp C_4–B^{K12}. Scale bars are 500 nm. (c,d) 4.0 kbp supercoiled dsDNA coated with (c) 0.375 ptn/bp of C_8–B^{Sso7d} and (d) 0.833 ptn/bp of C_4–B^{K12}. Scale bars are 400 nm. (e,f) Circular ssDNA from M13mp18 virus coated with (e) 1.45 ptn/bp of C_8–B^{Sso7d} and (f) 0.792 ptn/bp of C_4–B^{K12}. Scale bars are 500 nm. (g) Zoom of (a) for linear dsDNA+ C_8–B^{Sso7d}, showing a protein polymer bottle-brush structure around a DNA core. Scale bar is 150 nm. (h) Zoom of the square section of the C_8–B^{Sso7d} + ssDNA complex shown in (e), showing a short stretch of complex (arrow) for which the C_8–B^{Sso7d} protein polymer coating did not prevent intramolecular basepairing. Scale bar is 50 nm.

Table 1. Height and Contour Lengths of Protein Polymer Coated Linear 8 kbp dsDNA

		C_8–B^{Sso7d}					C_4–B^{K12}
ptn/bp	0	0.06	0.13	0.19	0.25	0.49	0.26
height (nm)	ND	0.61 ± 0.19	0.94 ± 0.18	1.09 ± 0.29	1.22 ± 0.26	1.21 ± 0.2	0.95 ± 0.19
contour length (nm)	2720[a]	ND	2382 ± 83	ND	2551 ± 65	2439 ± 36	2720 ± 32

[a]Theoretical contour length for bare linear 8 kbp dsDNA, ND: not determined.

Structures of Protein Polymer-Coated 1D DNA Templates from AFM Imaging. We used AFM imaging to investigate the nanoscale structure of complexes of the C_8–B^{Sso7d} protein polymers with a range of DNA templates: linear 8.0 kbp dsDNA, 4.0 kbp supercoiled dsDNA, and 7249 nt circular ssDNA (Figure 4a, 4c and 4e). For all templates, we compare the structures obtained with C_8–B^{Sso7d} with C_4–B^{K12} diblock polymer[13] for which DNA binding is purely electrostatic and not specific to DNA (Figure 4b, 4d and 4f). AFM images of complexes of C_8–B^{Sso7d} with 8.0 kb linear double stranded DNA are qualitatively similar to those formed with the C_4–B^{K12} diblock protein polymer (compare Figure 4a and b): the coating is homogeneous and preserves the contour length of the template. Upon increasing the protein to DNA ratio, the DNA molecules become progressively coated (Height in Table 1), without any indication of intramolecular aggregation. The bottle-brush architecture of the complexes can be observed in high resolution AFM images for complexes with C_8–B^{Sso7d} (Figure 4g). The C_8–B^{Sso7d} complexes have a somewhat larger height than the C_4–B^{K12} complexes. This most likely reflects both the larger and globular binding domain B^{Sso7d} and the larger length of the stabilizing C-block for C_8–B^{Sso7d}. A quantitative analysis (as described in the Materials and Methods section) also reveals that contour lengths of C_8–B^{Sso7d} complexes are significantly shorter than those of the bare DNA (Table 1). Indeed, it has been reported that Sso7d causes kinking that may reduce the effective contour length of dsDNA by 10–20%.[26]

For 4 kb supercoiled pDNA, complexation with C_8–B^{Sso7d} seems to lead to global opening up of plectonemic supercoils (Figure 4c) exposing its circular topology, possibly due to stiffening effects from the protein coating and due to induced twist of the topologically constrained DNA caused by protein binding. The complexes have a contour length of 1395 ± 29 nm, which is about the theoretical contour length of the naked pDNA (1360 nm, assuming a length of 0.34 nm per nt). B^{Sso7d} binding has been reported to lead to DNA unwinding through placement of its triple beta-sheet domain across the minor groove.[20,27] At a fixed linking number[28] this will be compensated by the introduction of positive supercoiling that balances part or all of the original negative supercoiling. The marked shortening of the apparent contour length of complexes that was observed for linear DNA is absent in the case of supercoiled pDNA. In clear contrast to complexation with C_8–B^{Sso7d}, the C_4–B^{K12} diblock leads to a tightening of plectonemic supercoils (Figure 4d), possibly *via* bridging of the opposing sides of a plectonemic supercoil by the binding domain. As a consequence, single thick contours are observed for C_4–B^{K12} pDNA complexes, that appear as flexible rod-like structures with a contour length that is close to half that of the contour length of bare pDNA, as previously reported.[13] For more images of the complexes of pDNA with both proteins, see the Supporting Information (Figure S3).

Complexes with single-stranded DNA are again markedly different for the two proteins (Figure 4e and f). It appears that the C_8–B^{Sso7d} protein polymer can almost completely prevent the formation of secondary structures due to intramolecular base pairing of the ssDNA. Therefore, it disentangles and stretches out the structure (Figure 4e and Supporting Information Figure S4). In most of the images a single short piece of an apparent duplex segment remains visible (marked segment with an arrow in Figure 4h) that could correspond to a local (nearly) palindromic sequence with particularly strong base pairing. The complexes with C_8–B^{Sso7d} have a contour length of 1326 ± 95 nm, which is 53.8% of the calculated contour length of naked ssDNA (2465 nm, assuming a

DOI: 10.1021/acsnano.6b05938
ACS Nano 2017, 11, 144–152

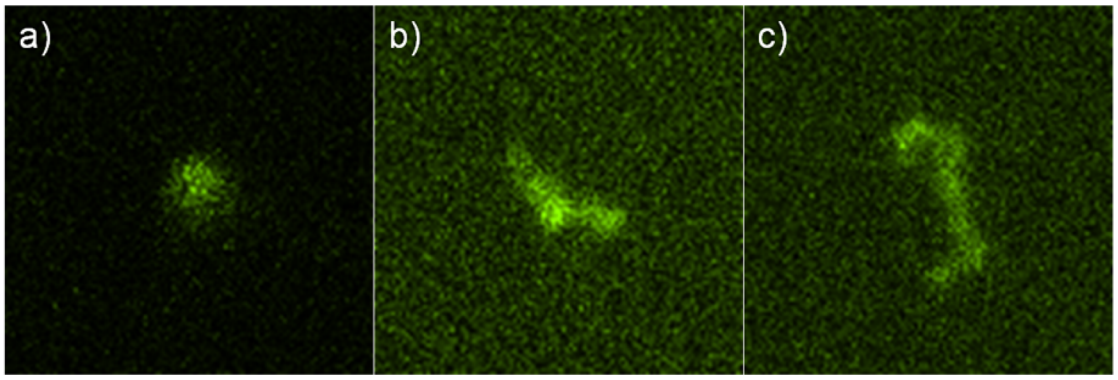

Figure 5. Increase of the coil size of T4 DNA upon binding C_8–B^{Sso7d} and C_4–B^{K12}. Representative snapshots of fluorescence microscope videos of T4 DNA that was (a) bare (b) coated with C_4–B^{K12} and (c) coated with C_8–B^{Sso7d}.

contourlength of 0.34 nm per nt). In clear contrast, the formation of secondary structures by intramolecular base pairing of the circular single-stranded M13mp18 virus DNA is not prevented in complexes with the diblock protein polymer C_4–B^{K12}. For that case, complexes have a collapsed and branched appearance (Figure 4f). Zooming in the C_8–B^{Sso7d} + ssDNA complexes (Figure 5a) shows a beaded appearance that is reminiscent of the "pearl-necklace" configurations we have found before[29] for complexes of C_4–B^{K12} with flexible polyanions. The prevention of intramolecular basepairing that we observe for ssDNA templates complexed with C_8–B^{Sso7d} (but not for C_4–B^{K12}) may be another advantage of using a binding domain that is DNA-specific.

Impact of Protein Polymer Coating on Hydrodynamic Radius of T4 DNA. For the C_4–B^{K12} diblock protein polymer, stiffening of linear dsDNA induced by the bottle-brush coating was previously studied using both AFM and nanochannel stretching experiments.[8] Here we qualitatively address stiffening of linear DNA by measuring changes in the translational diffusion constant (and hence the hydrodynamic radius) of linear double stranded T4 DNA (169 kbp) when it is coated with C_8–B^{Sso7d} and C_4–B^{K12}. Diffusion constants are deduced from the mean square displacements as a function of time (see Materials and Methods), by tracking the centers-of-mass of YOYO-1-stained T4 DNA using fluorescence microscopy. Representative images of bare T4 DNA, and T4 DNA coated with either C_4–B^{K12} or C_8–B^{Sso7d} are shown in Figure 5. Estimated diffusion coefficients D and the corresponding hydrodynamic radii R_H of bare T4 DNA, and T4 DNA coated with C_8–B^{Sso7d} and C_4–B^{K12} are given in Table 2. Bare T4 DNA appears more compact (Figure 5a), rotates more rapidly, and diffuses faster than T4 DNA coated with C_4–B^{K12} (Figure 5b) or C_8–B^{Sso7d} protein polymers (Figure 5c). Especially when T4-DNA is coated with C_8–B^{Sso7d}, the DNA molecules are quite extended and a coarse linear contour can typically be distinguished. In the videos it appears to diffuse more slowly (Supporting Videos S1–S3). C_4–B^{K12} has a similar effect but the decrease in mobility and the stretching is less pronounced. Hydrodynamic radii deduced from the estimated diffusion constants are roughly twice larger for C_8–B^{Sso7d} coated than for bare T4 DNA. In no case aggregation was detected. While the hydrodynamic radius of the (coated) T4 DNA mainly reflects the stiffness of the coated DNA, it is also sensitive (to a lesser extent) to the thickness of the bottle-brush coating, and to excluded volume effects between the bottle-brush coated DNA segments. Therefore, while it is clear that, like the C_4–B^{K12} coating, the C_8–B^{Sso7d} coating leads to a significant stiffening of the DNA, more detailed studies will have to be performed to precisely quantify the induced stiffening, and to determine whether it is larger or smaller than what we have previously found for C_4–B^{K12}.

Table 2. Diffusion Constants D and Hydrodynamic Radii R_H of T4 DNA, Coated with C_4–B^{K12} and C_8–B^{Sso7d}

	bare	C_4–B^{K12}	C_8–B^{Sso7d}
D [10^{-13} m^2/s]	3.50 ± 0.09	2.42 ± 0.04	1.73 ± 0.07
R_H [μm]	0.70 ± 0.02	1.007 ± 0.02	1.41 ± 0.06

Protein Polymer Coating of DNA Origami Nanostructures. Next we move on to the coating of more complicated DNA templates, viz. self-assembled DNA nanostructures. Specifically, we will use DNA origami, which is based on the programmed formation of Holliday junctions[30] between M13mp18 viral ssDNA scaffold and small synthetic ssDNA staple strands. The specific structure that we will work with is the "tall rectangle" structure designed by Paul Rothemund.[31] We first characterize the binding isotherms of the protein polymers when binding to the two-dimensional origami DNA templates using an electrophoretic mobility shift assay (EMSA) using agarose gel electrophoresis.

Results are shown in Figure 6. We find that the addition of the protein polymers reduces the electrophoretic mobility of the DNA origami, much like the behavior of the other DNA templates, again confirming the generic affinity of the protein polymers for DNA templates. For complexes of DNA origami with the C_4–B^{K12} protein polymer, mobility begins to decrease at around 0.054 ptn/bp, and saturates at around 0.861 ptn/bp (Figure 6a). For complexes of DNA origami with the C_8–B^{Sso7d} protein polymer (Figure 6b), the mobility is already reduced at much lower protein polymer concentrations, namely, at 0.008 ptn/bp. The mobility shift also saturates at a much lower protein polymer concentration, namely at around 0.094 ptn/bp. Approximate binding curves deduced from the EMSA data is shown in Figure 6c. The different binding behavior for the two protein polymers most likely arises from the fact that the Sso7d binding domain is DNA specific, whereas, as discussed above, the K_{12} domain binds through electrostatic interactions alone, and is not DNA-specific.

Next, using AFM we investigated the spatial structures of complexes of the protein polymers with the DNA origami. Results are shown in Figure 7. Coating DNA origami with the C_8–B^{Sso7d} preserves the designed structure of the DNA

DOI: 10.1021/acsnano.6b05938
ACS Nano 2017, 11, 144–152

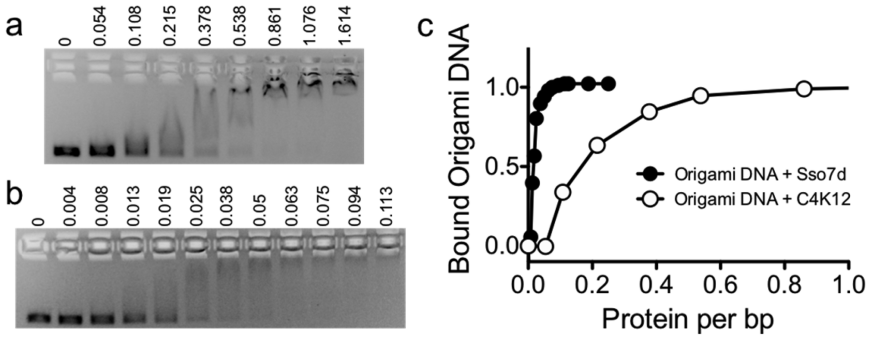

Figure 6. Binding of protein polymers to DNA origami nanostructures. Electrophoretic mobility shift assay for (a) 7.2 kbp "tall rectangle" DNA origami[31] complexed with C_4–B^{K12} and (b) C_8–B^{Sso7d}. Protein/DNA bp ratios are shown at the top. (c) Bound DNA as a function of Protein/DNA bp ratio.

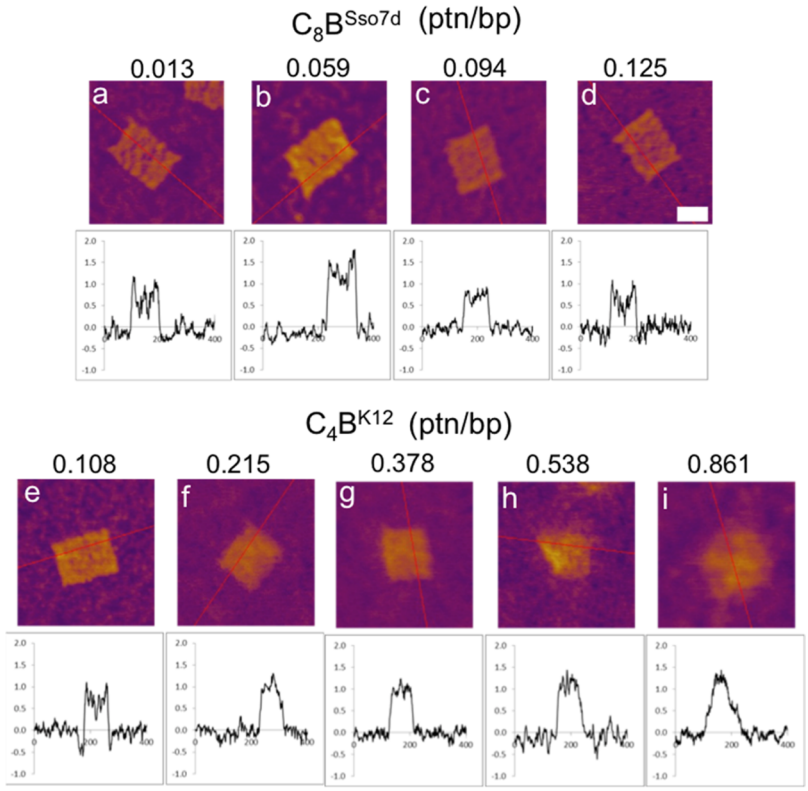

Figure 7. AFM images of complexes formed with single 2D DNA origami templates. Atomic force microscopy images and corresponding height maps of DNA origami coated with C8-BSso7d (top row) at ptn/bp ratio of (a) 0.013 ptn/bp, (b) 0.059 ptn/bp, (c) 0.094 ptn/bp, (d) 0.125 ptn/bp; and with C4-BK12 (bottom row) at ptn/bp ratio of (e) 0.108 ptn/bp, (f) 0.215 ptn/bp, (g) 0.378 ptn/bp, (h) 0.538 ptn/bp, (i) 0.861 ptn/bp. Scale bar is 50 nm.

origami, as can be seen in Figure 7a–d. In contrast, coating DNA origami with C_4–B^{K12} produces distorted origami structures at high ptn/bp ratios (Figures 7e–i). Note that lower protein polymer concentrations were used for C_8–B^{Sso7d} than for C_4–B^{K12}, in view of the much lower concentration needed to saturate binding for the C_8–B^{Sso7d} protein polymer. This may also have helped in preventing structural distortion of the coated DNA origami for the case of coating with C_8–B^{Sso7d}. It is also interesting to notice that the height of the coated origami seems not to increase when more protein is added. This effect can be because the hydrophilic domain is quite flexible and could flatten out on and around the DNA origami and remain sufficiently dynamic that it is difficult to observe on top of the origami.

Enzymatic Accessibility of Coated DNA. Accessibility of macromolecular agents to DNA coated by molecules such as proteins or other polymers is relevant for a wide range of possible applications. As a way to estimate the DNA accessibility, we evaluated the ability of the C_8–B^{Sso7d} protein to protect the DNA from degradation by nuclease enzymes (Figure 8, electrophoresis gel images given in Supporting Information Figure S5). Solutions containing pDNA or DNA origami complexed with C_8–B^{Sso7d} or C_4–B^{K12} were incubated with a high concentration of DNase I, a nonsequence specific endonuclease enzyme. At different incubation times aliquots of the sample were taken and the reaction quenched with EDTA. The samples were then run in an agarose gel. The intensity of the band corresponding to the protein–DNA complex was quantified with the ImageJ software and plotted against time.

DOI: 10.1021/acsnano.6b05938
ACS Nano 2017, 11, 144–152

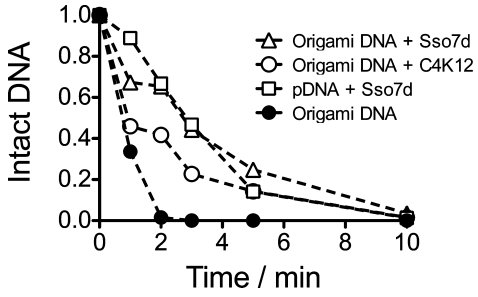

Figure 8. Protection of pDNA and origami DNA against digestion by DNase I by protein polymer coating. Fraction intact DNA as a function of incubation time for pDNA and origami DNA coated with either C8-BSso7d or C4-BK12 at a protein to DNA bp ratio of 0.188 ptn/bp.

The experiment shows that the protein polymer coating offers a moderate degree of protection against nucleases for both DNA origami and pDNA. Coated templates are degraded in about 10 min, which is about 5 times slower than the bare DNA templates (see the curve for bare origami DNA in Figure 8). Protection by C_8–B^{Sso7d} is somewhat stronger than by C_4–B^{K12}, possibly due to the longer hydrophilic brush and the DNA-specific binding domain.

CONCLUSIONS

We have shown that we can harness the high specificity and affinity of naturally occurring DNA binding domains in combination with a long unstructured domain for controlled binding and coating of a wide range of different types of DNA templates, including DNA origami nanostructures. Using the binding properties of the designed protein C_8–B^{Sso7d}, we can modulate physical-chemical properties of DNA templates such as their stiffness, surface chemistry and accessibility to enzymes. In comparison to the C_4–B^{K12} protein polymer that only binds through nonspecific electrostatics, the Sso7d DNA-binding domain of the C_8–B^{Sso7d} protein polymer has advantages of resulting in stable coatings at lower protein concentrations, prevention of intramolecular bridging in ssDNA and supercoiled pDNA templates, and preservation of shape of DNA origami nanostructures. Also, the B^{Sso7d} domain will be less sensitive to undesired molecular cross-talk with other negatively charged surfaces or polyelectrolytes. Additionally, the B^{Sso7d} is extremely stable itself, and also stabilizes DNA against thermal denaturation.[16] While for now, we have not yet zoomed in on a specific application, it is clear that the modular and recombinant nature of the C_8–B^{Sso7d} protein polymer allows for very precise modifications for specific applications, *e.g.*, cell-binding domains[34] that would promote the transfection of individual coated DNA nanostructures, or material-binding domains[35] and in this way contribute to the convergence of protein and DNA nanotechnologies.

MATERIALS AND METHODS

Materials. Linear 8.0, 2.5, and 2.0 kbp dsDNA were purchased from Thermo Scientific (Waltham, MA, USA). M13mp18 single-stranded DNA 7249 nt (ssDNA) was purchased from New England Biolabs (Ipswich, MA, USA) and T4-DNA were purchased from Nippon Gene (Tokyo, Japan) and used without further purification, supercoiled 4.0 and 2.7 kbp pDNA were recovered from recombinant *E. coli* by using the GeneJet plasmid Miniprep kit from Thermo Scientific. All short ssDNA staples used for DNA origami formation were purchased from IDT (Integrated DNA Technologies, Inc.). The precise sequence of staples and scaffold/staple layout for the "Tall Rectangle" design can be found in ref 31. YOYO-1 was purchased from Invitrogen (Life Technologies, Carlsbad, CA, USA). Restriction enzymes were purchased from New England Biolabs or from Thermo Scientific. The C_4–B^{K12} and C_4 protein polymers were produced and purified following previously published methods[13,14]

Molecular Cloning. A double-stranded adapter encoding the Sso7d binding domain (B^{sso7d}) was prepared by annealing of overlapping codon-optimized oligonucleotides (Eurogentec, Belgium; Supporting Information Table S1). The vector containing the DNA coding for the hydrophilic random coil protein "C_8" was prepared in the following way: a fragment C_4, obtained from plasmid pMTL23-C_4 (see ref 14) by double digestion with the restriction enzymes *DraIII*/*Van91I*, was ligated into the plasmid pMTL23-C_4 previously digested with *Van91I* to obtain pMTL23-C_8. The plasmid pMTL23-C_8–B^{Sso7d} was obtained by ligating the double-stranded B^{Ss07d} adapter into the vector pMTL23-C_8 previously digested with restriction enzymes *Van91I* and *Eco*RI. The fragment encoding the C_8–B^{Sso7d} protein-based polymer was released through digestion of plasmid pMTL23-C_8–B^{Sso7d} with *Xho1*/*Eco*RI and ligated into the correspondingly digested *P. pastoris* expression vector pPIC9 (Invitrogen). The resulting plasmid pPIC9-C^8–B^{Sso7d} was linearized with *Sal*I and electroporated into *P. pastoris* strain GS115 (Invitrogen). The plasmid integrates into the genome through homologous recombination at the *his4 locus* providing normal growth on methanol. The presence of the genes was verified by polymerase chain reaction.

Biosynthesis of Protein. The fermentation was similar to the previously described method.[13] Fed-batch fermentations using minimal basal salts medium were performed in 2.5-L Bioflo 3000 fermentors (New Brunswick Scientific, Edison, NJ). The methanol fed-batch phase for protein production lasted 2–3 days. A homemade semiconductor gas sensor–controller was used to monitor the methanol level in the off-gas and to maintain a constant level of 0.2% (w/v) methanol in the broth. The pH was maintained at 3.0 throughout the fermentation by addition of ammonium hydroxide. At the end of the fermentation, the cells were separated from the broth by centrifugation for 15 min at 10 000*g* (room temperature or 4 °C) in an SLA-3000 rotor (Thermo Scientific, Waltham, MA), and the supernatant was microfiltered (Pall Corporation, Port Washington, NY) and stored at 4 °C for subsequent purification.

Protein Purification. All centrifugation was done for 30 min at 20 000*g* at 4 °C, interchangeably in a Sorvall SLA-1500 or SLA-3000 rotor (Thermo Scientific, Waltham, MA). First, medium salts were removed from the cell-free broth by adjustment of the pH to 8.0 with NaOH, followed by centrifugation. Subsequently, the protein-based polymer was selectively precipitated from the solution by adding ammonium sulfate to a saturation of 45%, incubating overnight at 4 °C, and subsequent centrifugation. The pellet was resuspended in an equal volume (relative to the cell-free broth) of Milli-Q water and precipitation was repeated once at 4 °C, using an overnight incubation. The pellet was resuspended in 0.2 volumes (relative to the cell-free broth) of Milli-Q water and sodium chloride and acetone were added to a final concentration of 50 mM and 40% (v/v), respectively. After centrifugation the acetone concentration of the supernatant was raised to 80% (v/v), and the solution was centrifuged to precipitate the pure protein-based polymer. The pellet was dried overnight, resuspended in Milli-Q water, extensively desalted by dialysis against Milli-Q water using a using Spectra/Por 7 tubing (Spectrum Laboratories) with a 1 kDa molecular weight cutoff, and lyophilized.

SDS-PAGE and MALDI-TOF. SDS-PAGE was carried out using the NuPAGE Novex system (Invitrogen, Carlsbad, CA) with 10% Bis-Tris gels, 2-(*N*-morpholino)ethanesulfonic acid (MES)–SDS as running buffer, and SeeBlue Plus2 prestained molecular mass markers. Gels were stained with Coomassie SimplyBlue SafeStain (Invitrogen). MALDI-TOF mass spectrometry was carried out in an Ultraflex mass spectrometer (Bruker, Billerica, MA). Protein samples were prepared by the dried droplet method. The matrix was made up of 2.5-dihydroxyacetophenone (5 mg mL^{-1}), diammonium hydrogen citrate (1.5 mg mL^{-1}), 25% (v/v) ethanol, and 1% (v/v) trifluoroacetic acid on an AnchorChip target (600 μm, Bruker). An external mass

DOI: 10.1021/acsnano.6b05938
ACS Nano 2017, 11, 144–152

calibration was done based on Protein Calibration Standard II (Bruker).

Preparation of Protein−DNA Complexes. Protein−DNA complexes dissolved in 10 mM sodium phosphate buffer, pH 7.4, were prepared by mixing of pipetted portions of DNA stock solution, protein stock solution and 100 mM phosphate buffer, pH 7.4, in Milli-Q water. Mixtures were vortexed for 1 min. Volumes of the mixed portions of stock DNA and protein solutions were varied according to their initial concentration and the desired final molar protein/DNA-bp (ptn/bp) ratio. Protein stock solutions were prepared just before use by dissolving a weighted amount of lyophilized protein in Milli-Q water.

Preparation of DNA Origami. To assemble the tall rectangle DNA origami designed by Rothemund,[31] 5 nM single-stranded M13mp18 DNA (NEB, 7249 nt long) was mixed in 1× TAEMg (40 mM Tris, 20 mM Acetic acid, 2 mM EDTA and 12.5 mM Magnesium acetate, pH 8.0) with 50 nM staple strands. The solution was heated to 80 °C and then cooled to 20 °C over 2 h and subsequently kept at 4 °C.

Preparation of Protein−DNA Origami Complexes. Protein−DNA origami complexes were prepared by mixing of pipetted portions of DNA origami stock solution in 1× TAEMg (40 mM Tris, 20 mM Acetic acid, 2 mM EDTA and 12.5 mM Magnesium acetate, pH 8.0) and protein stock solution in 10 mM acetate buffer, pH 4.85. Mixtures were vortexed for 10 s. Volumes of the mixed portions of stock DNA and protein solutions were varied according to their initial concentration and the desired final protein/DNA-bp (ptn/bp) ratio.

Electrophoretic Mobility Shift Assay (EMSA). Aliquots of DNA (50 ng/μL for pDNA and 2.0 kb linear dsDNA and 30 ng/μL for circular M13 ssDNA) were mixed with different volumes of a C_8−B^{Sso7d} solution (0.035 or 0.35 g L^{-1}) and with 10× Tris−acetate−EDTA (TAE) buffer (pH 8) for a final volume of 10 μL. After incubation for at least 60 min at room temperature, the mixtures were mixed with 6× loading buffer and 10−12 μL of the final mixture were subjected to electrophoresis in an agarose gel (1%) for at least 60 min at 95 V using 1× TAE buffer (pH 8). Bands were visualized using Sybr gold. In the case of DNA origami, aliquots of 5 nM origami (40 ng/μL) in 1× TAEMg (40 mM Tris, 20 mM Acetic acid, 2 mM EDTA and 12.5 mM Magnesium acetate, pH 8.0) were mixed with different volumes of a C_8−B^{Sso7d} solution (0.05 to 0.2 g L^{-1}) in 10 mM acetate buffer, pH 4.85. Mixtured for vortexed for 10 s and then incubated for 60 min at room temperature. The mixtures were mixed with 6× loading buffer and subjected to electrophoresis in an agarose gel (1%) for 30 min at 90 V using 1× TAEMg buffer. Bands were visualized using ethidium bromide.

Fluorescence Quenching. Protein + dsDNA sample were incubated between 1 and 4h at room temperature before measuring the fluorescence intensity in a Cytation 3 imaging reader (Biotek). For fluorescence measurements, 150 μL of sample were deposited in a 96-well Greiner 96 Black Flat Bottom Fluotrac. Using top optics, samples were excited at 285 nm and fluorescence emission was measured between 314 and 400 nm in 2 nm steps. Fluorescence emission at 340 nm was plotted after buffer subtraction.

Atomic Force Microscopy. Approximately 3−5 μL DNA−protein solution was added to clean hydrophilic silicon (1 × 1 cm) and left for 2 min. Then it was rinsed with filtered Milli-Q water (1 mL) to remove salts and non absorbed particles, followed by soaking up of excess water using a tissue and slow drying under a N_2 stream. Samples were analyzed using a Digital Instruments NanoScope V equipped with a silicon nitride probe (Bruker, MA, USA) with a spring constant of 0.4 N m^{-1} in ScanAsyst imaging mode. Images were recorded with >0.965 Hz and 1024 samples per line. Image processing was done with NanoScope Analysis 1.20 software. Contour length and long axis length measurements were performed manually with the help of the ImageJ software. In the case of DNA origami, 1 μL of 5 nM DNA origami-protein-based polymer complex solution was mixed with 9 μL of filtered Milli-Q water and immediately added to a freshly cleaved mica surface (1 cm diameter) and left for 3 min. Then it was rinsed with 50 μL of filtered Milli-Q water for 2 s to remove salts and nonabsorbed particles, followed by slow drying under a N_2 stream. Samples were analyzed using an Asylum Cypher equipped with a silicon BioLever Mini probe (Olympus) with a spring constant of 0.25 N m^{-1} in AC Molecule tapping mode. Images were recorded at 1.95 Hz and 512 samples per line. Height profile measurements were performed with Igor software.

Fluorescence Microscopy Imaging. Protein-coated single T4-DNA molecules were stained at room temperature with the intercalating fluorescent dye YOYO-1 in 10 mM Tris-HCl, pH 8.0 (intercalation ratio of one every 25 bp). The samples were incubated at least 30 min and the final T4-DNA concentration was ∼5 μg/mL. The fluorescent protein−DNA was imaged with a Nikon Eclipse Ti inverted fluorescence microscope equipped with a 200 W metal halide lamp, a filter set and a 100× oil immersion objective. The exposure time was controlled using an UV light shutter and the images were collected with an electron multiplying charge-coupled device (EMCCD) camera (Andor iXon X3). The diffusion coefficient and hydrodynamic radius of bare T4 DNA, and T4 DNA and coated with C_4−B^{K12} (0.834 ptn/bp) and C_8−B^{Sso7d} (0.5 ptn/bp) were calculated from processing videos of at least 1 min duration using previously reported algorithms in MatLab.[32,33] The samples were incubated at least 30 min and the final T4-DNA concentration used for the experiments was ∼5 μg/mL.

DNA Protection Test. pDNA 2.6 kbp (concentration of 19.7 ng/μL) was complexed with C_8−B^{Sso7d} (concentration 0.44 mg/mL) in TAE buffer (pH 8) for 1h at room temperature (0.188 ptn/bp). Then 1 μL of the enzyme DNase I (RNase free, Thermo Scientific) 0.055 U was added to 35.5 μL complexes dissolved in reaction DNase I buffer (100 mM Tris-HCl, pH 7.5, 25 mM $MgCl_2$, 1 mM $CaCl_2$) for a final [DNA] = 17.2 μg/mL and immediately incubated at 25 °C using a thermo block. Aliquots of 3.5 μL were taken at different times and mixed with 3.5 μL of EDTA 50 mM. After addition of loading buffer (6×) the sample was electrophoresed in agarose gel 1% at 100 V for 45 min. DNA bands were visualized using ethidium bromide. The same procedure was repeated for DNA Origami 7.2 kbp (concentration 20 ng/μL). To estimate fractions of intact DNA as a function of time, gel images were analyzed using the ImageJ software.

ASSOCIATED CONTENT

Supporting Information

The Supporting Information is available free of charge on the ACS Publications website at DOI: 10.1021/acsnano.6b05938.

Extra methods and Supporting Figures S1−S5 (PDF)
Video S1 (AVI)
Video S2 (AVI)
Video S3 (AVI)

AUTHOR INFORMATION

Corresponding Authors

*E-mail: armaquim@gmail.com.
*E-mail: renko.devries@wur.nl.

ORCID

Armando Hernandez-Garcia: 0000-0001-5505-3423
Thomas H. LaBean: 0000-0002-6739-2059

Present Address

#Simpson Querrey Institute, Northwestern University, Chicago, Illinois, United States.

Notes

The authors declare no competing financial interest.

ACKNOWLEDGMENTS

R. de Vries and A. Hernandez-Garcia acknowledge financial support of the Dutch Polymer Institute, project 698. A. Hernandez-Garcia acknowledges financial support of CONACYT, Mexico (scholarship for graduate studies). Financial support to M. W. T. Werten, F. A. de Wolf and M. A. Cohen

DOI: 10.1021/acsnano.6b05938
ACS Nano 2017, 11, 144−152

Stuart is provided by ERC Advanced Grant 267254 "BioMate". T. H. LaBean and N. A. Estrich acknowledge financial support from the National Science Foundation through NSF-ECCS-EPMD-1231888. We thank Inge Storm, for performing the fermentation and purification of some of the protein polymer C_4–B^{K12} material used in this study.

REFERENCES

(1) Andersen, E. S.; Dong, M.; Nielsen, M. M.; Jahn, K.; Subramani, R.; Mamdouh, W.; Golas, M. M.; Sander, B.; Stark, H.; Oliveira, C. L. P.; Pedersen, J. S.; Birkedal, V.; Besenbacher, F.; Gothelf, K. V.; Kjems, J. Self-assembly of a Nanoscale DNA Box with a Controllable Lid. *Nature* **2009**, *459*, 73–U75.

(2) Lee, H.; Lytton-Jean, A. K. R.; Chen, Y.; Love, K. T.; Park, A. I.; Karagiannis, E. D.; Sehgal, A.; Querbes, W.; Zurenko, C. S.; Jayaraman, M.; Peng, C. G.; Charisse, K.; Borodovsky, A.; Manoharan, M.; Donahoe, J. S.; Truelove, J.; Nahrendorf, M.; Langer, R.; Anderson, D. G. Molecularly Self-assembled Nucleic Acid Nanoparticles for Targeted *in vivo* siRNA Delivery. *Nat. Nanotechnol.* **2012**, *7*, 389–393.

(3) Douglas, S. M.; Dietz, H.; Liedl, T.; Hogberg, B.; Graf, F.; Shih, W. M. Self-Assembly of DNA into Nanoscale Three-Dimensional Shapes. *Nature* **2009**, *459*, 414–418.

(4) LaBean, T. H.; Li, H. Y. Constructing Novel Materials with DNA. *Nano Today* **2007**, *2*, 26–35.

(5) Hamon, L. C.; Pastré, D.; Dupaigne, P.; Breton, C. L.; Cam, E. L.; Piétrement, O. High-Resolution AFM Imaging of Single-Stranded DNA-binding (SSB) Protein-DNA Complexes. *Nucleic Acids Res.* **2007**, *35*, e58.

(6) Bensimon, A.; Simon, A.; Chiffaudel, A.; Croquette, V.; Heslot, F.; Bensimon, D. Alignment and Sensitive Detection of DNA by a Moving Interface. *Science* **1994**, *265*, 2096–2098.

(7) Lam, E. T.; Hastie, A.; Lin, C.; Ehrlich, D.; Das, S. K.; Austin, M. D.; Deshpande, P.; Cao, H.; Nagarajan, N.; Xiao, M.; Kwok, P. Y. Genome Mapping on Nanochannel Arrays for Structural Variation Analysis and Sequence Assembly. *Nat. Biotechnol.* **2012**, *30*, 771–776.

(8) Zhang, C.; Hernandez-Garcia, A.; Jiang, K.; Gong, Z.; Guttula, D.; Ng, S. Y.; Malar, P. P.; van Kan, J. A.; Dai, L.; Doyle, P. S.; Vries, R. d.; van der Maarel, J. R. C. Amplified Stretch of Bottlebrush-coated DNA in Nanofluidic Channels. *Nucleic Acids Res.* **2013**, *41*, e189.

(9) Michalet, X.; Ekong, R.; Fougerousse, F.; Rousseaux, S.; Schurra, C.; Hornigold, N.; vanSlegtenhorst, M.; Wolfe, J.; Povey, S.; Beckmann, J. S.; Bensimon, A. Dynamic Molecular Combing: Stretching the Whole Human Genome for High-Resolution Studies. *Science* **1997**, *277*, 1518–1523.

(10) Hall, A. R.; van Dorp, S.; Lemay, S. G.; Dekker, C. Electrophoretic Force on a Protein-Coated DNA Molecule in a Solid-State Nanopore. *Nano Lett.* **2009**, *9*, 4441–4445.

(11) Kumar, H.; Lansac, Y.; Glaser, M. A.; Maiti, P. K. Biopolymers in Nanopores: Challenges and Opportunities. *Soft Matter* **2011**, *7*, 5898–5907.

(12) Yeo, L. Y.; Chang, H. C.; Chan, P. P. Y.; Friend, J. R. Microfluidic Devices for Bioapplications. *Small* **2011**, *7*, 12–48.

(13) Hernandez-Garcia, A.; Werten, M. W. T.; Stuart, M. C.; de Wolf, F. A.; de Vries, R. Coating of Single DNA Molecules by Genetically Engineered Protein Diblock Copolymers. *Small* **2012**, *8*, 3491–3501.

(14) Werten, M. W. T.; Wisselink, W. H.; Jansen-van den Bosch, T. J.; de Bruin, E. C.; de Wolf, F. A. Secreted Production of a Custom-designed, Highly Hydrophilic Gelatin in Pichia Pastoris. *Protein Eng., Des. Sel.* **2001**, *14*, 447–454.

(15) Baumann, H.; Knapp, S.; Lundback, T.; Ladenstein, R.; Hard, T. Solution Structure and DNA-binding Properties of a Thermostable Protein from the Archaeon Sulfolobus Solfataricus. *Nat. Struct. Biol.* **1994**, *1*, 808–819.

(16) Baumann, H.; Knapp, S.; Karshikoff, A.; Ladenstein, R.; Härd, T. DNA-binding Surface of the Sso7d Protein from Sulfolobus Solfataricus. *J. Mol. Biol.* **1995**, *247*, 840–846.

(17) Gao, Y. G.; Su, S. Y.; Robinson, H.; Padmanabhan, S.; Lim, L.; McCrary, B. S.; Edmondson, S. P.; Shriver, J. W.; Wang, A. H. J. The Crystal Structure of the Hyperthermophile Chromosomal Protein Sso7d Bound to DNA. *Nat. Struct. Biol.* **1998**, *5*, 782–786.

(18) Edmondson, S. P.; Shriver, J. W. DNA-binding Proteins Sac7d and Sso7d from Sulfolobus. *Methods Enzymol.* **2001**, *334*, 129–145.

(19) Consonni, R.; Arosio, I.; Belloni, B.; Fogolari, F.; Fusi, P.; Shehi, E.; Zetta, L. Investigations of Sso7d Catalytic Residues by NMR Titration Shifts and Electrostatic Calculations. *Biochemistry* **2003**, *42*, 1421–1429.

(20) Agback, P.; Baumann, H.; Knapp, S.; Ladenstein, R.; Hard, T. Architecture of Nonspecific Protein-DNA Interactions in the Sso7d-DNA Complex. *Nat. Struct. Biol.* **1998**, *5*, 579–584.

(21) Wang, Y.; Prosen, D. E.; Mei, L.; Sullivan, J. C.; Finney, M.; Vander Horn, P. B. A Novel Strategy to Engineer DNA Polymerases for Enhanced Processivity and Improved Performance *in vitro*. *Nucleic Acids Res.* **2004**, *32*, 1197–1207.

(22) Gera, N.; Hill, A. B.; White, D. P.; Carbonell, R. G.; Rao, B. M. Design of pH Sensitive Binding Proteins from the Hyperthermophilic Sso7d Scaffold. *PLoS One* **2012**, *7*, 14.

(23) Gera, N.; Hussain, M.; Wright, R. C.; Rao, B. M. Highly Stable Binding Proteins Derived from the Hyperthermophilic Sso7d Scaffold. *J. Mol. Biol.* **2011**, *409*, 601–616.

(24) Hardy, C. D.; Martin, P. K. Biochemical Characterization of DNA-binding Proteins from Pyrobaculum Aerophilum and Aeropyrum Pernix. *Extremophiles* **2008**, *12*, 235–246.

(25) Robinson, H.; Gao, Y. G.; McCrary, B. S.; Edmondson, S. P.; Shriver, J. W.; Wang, A. H. J. The Hyperthermophile Chromosomal Protein Sac7d Sharply Kinks DNA. *Nature* **1998**, *392*, 202–205.

(26) Driessen, R. P. C.; Meng, H.; Suresh, G.; Shahapure, R.; Lanzani, G.; Priyakumar, U. D.; White, M. F.; Schiessel, H.; van Noort, J.; Dame, R. T. Crenarchaeal Chromatin Proteins Cren7 and Sul7 Compact DNA by Inducing Rigid Bends. *Nucleic Acids Res.* **2013**, *41*, 196–205.

(27) Napoli, A.; Zivanovic, Y.; Bocs, C.; Buhler, C.; Rossi, M.; Forterre, P.; Ciaramella, M. DNA Bending, Compaction and Negative Supercoiling by the Architectural Protein Sso7d of Sulfolobus Solfataricus. *Nucleic Acids Res.* **2002**, *30*, 2656–2662.

(28) Bates, A. D.; Maxwell, A. *DNA Topology*; Oxford University Press: Oxford, 2005; p 216.

(29) Golinska, M. D.; de Wolf, F.; Stuart, M. A. C.; Hernandez-Garcia, A.; de Vries, R. Pearl-Necklace Complexes of Flexible Polyanions with Neutral-Cationic Diblock Copolymers. *Soft Matter* **2013**, *9*, 6406–6411.

(30) Eichman, B. F.; Vargason, J. M.; Mooers, B. H. M.; Ho, P. S. The Holliday Junction in an Inverted Repeat DNA Sequence: Sequence Effects on the Structure of Four-Way Junctions. *Proc. Natl. Acad. Sci. U. S. A.* **2000**, *97*, 3971–3976.

(31) Rothemund, P. W. K. Folding DNA to Create Nanoscale Shapes and Patterns. *Nature* **2006**, *440*, 297–302.

(32) Kundukad, B.; van der Maarel, J. R. C. Control of the Flow Properties of DNA by Topoisomerase II and Its Targeting Inhibitor. *Biophys. J.* **2010**, *99*, 1906–1915.

(33) Zhu, X. Y.; Kundukad, B.; van der Maarel, J. R. C. Viscoelasticity of Entangled Lambda-Phage DNA Solutions. *J. Chem. Phys.* **2008**, *129*, 185103.

(34) Gray, B. P.; Brown, K. C. Combinatorial Peptide Libraries: Mining for Cell-Binding Peptides. *Chem. Rev.* **2014**, *114*, 1020–1081.

(35) Care, A.; Bergquist, P. L.; Sunna, A. Solid-binding Peptides: Smart tools for Nanobiotechnology. *Trends Biotechnol.* **2015**, *33*, 259–268.

DOI: 10.1021/acsnano.6b05938
ACS Nano 2017, 11, 144–152